Polymer(Korea), Vol. 41, No. 3, pp. 514-523 (2017)
https://doi.org/10.7317/pk.2017.41.3.514

ISSN 0379-153X(Print)
ISSN 2234-8077(Online)

폴리프로필렌/열가소성 폴리에스터 엘라스토머 블렌드의 제조 및 물성

김영곤 · 김영선 · 최진규 · 백성현 · 심상은†
인하대학교 화학 및 화학공학 융합대학원
(2016년 11월 19일 접수, 2016년 12월 22일 수정, 2017년 1월 2일 채택)

Preparation and Properties of Polypropylene/Thermoplastic Polyester Elastomer Blends

Yeong Gon Kim, Yeongseon Kim, Jin Kyu Choi, Sung-Hyeon Baeck, and Sang Eun Shim†
Department of Chemistry & Chemical Engineering, Inha University, 253 Yonghyundong, Namgu, Incheon 22212, Korea
(Received November 19, 2016; Revised December 22, 2016; Accepted January 2, 2017)

초록: 폴리프로필렌/열가소성 폴리에스터 엘라스토머(PP/TPEE) 블렌드를 제조하였다. 두 상의 상용성을 증가시키기 위하여 maleic anhydride-grafted polypropylene(MA-*g*-PP)를 배합 도중 첨가하였다. SEM을 통한 모폴로지 분석 결과, 두 상은 상용성이 없었으며 MA-*g*-PP를 첨가한 결과 상용성이 발현되어 MA-*g*-PP가 효과적인 상용화제로 작용하였다. MA-*g*-PP를 첨가한 PP/TPEE 블렌드는 XRD 분석 결과 20.9° 피크의 강도가 증가하였으며 21.6° 피크는 점차적으로 감소하였다. 상용화제가 첨가된 경우의 기계적 물성 증가는 SEM 및 XRD의 분석 결과와 부합하였다. DSC 분석 결과, TPEE의 함량이 증가할수록 결정화도가 감소하였으며 MA-*g*-PP가 첨가된 경우 상용성으로 인하여 단일의 유리전이온도가 관찰되었으며 열적 안정성이 증가되었다.

Abstract: Polypropylene (PP)/thermoplastic polyester elastomer (TPEE) blends were prepared. To enhance the compatibility between the two phases, maleic anhydride-grafted polypropylene (MA-*g*-PP) was applied during melt-mixing. The morphology obtained from scanning electron microscopy (SEM) showed that TPEE was not miscible with PP, however, those of the PP/TPEE/MA-*g*-PP indicated that PP and TPEE turned to miscible because MA-*g*-PP served as an effective compatibilizer. The tensile tests confirmed that the tensile strength of the PP/TPEE blends decreased and the elongation increased with increasing TPEE content. The increase in tensile strength of the PP/TPEE/MA-*g*-PP blends was associated with the morphology shown by SEM and internal structure. X-ray diffraction (XRD) confirmed that compared to the PP/TPEE blend, the intensity of the 20.9° peak of the PP/TPEE/MA-*g*-PP increased and that of the 21.6° peak decreased gradually due to the MA-*g*-PP. In differential scanning calorimetry (DSC), the crystallinity (X_c) of the PP/TPEE blends decreased with increasing TPEE content. The PP/TPEE/MA-*g*-PP blends showed a single weak glass transition (T_g) peak due to the compatibility between the PP and TPEE. The thermal stability of the PP/TPEE blends with MA-*g*-PP was also higher than that of the PP/TPEE.

Keywords: polypropylene, thermoplastic polyester elastomer, blends, compatibilizer.

Introduction

Thermoplastic elastomers (TPE) are new materials having both elastic and plastic properties. Among the TPEs, a thermoplastic polyester elastomer (TPEE), which consists of poly(butylene terephthalate) (PBT) as a hard segment and poly(tetramethylene ether glycol terephthalate) as a soft segment (Figure 1), has superior mechanical, thermal properties, and elasticity.[1,2] It has attracted a great deal of interest due to its low specific gravity and exceptional recyclability, which has been considered as the eco-friendly material that replaces vulcanized rubber and poly(vinyl chloride) (PVC). Therefore, in both academic and commercial fields, many researches on the modification of TPEE have progressed in order to attain its more suitable properties for various applications such as electronic instruments, automotive parts, clothes, and outdoor instruments, etc.

Block and graft copolymerization are ideal methods for

†To whom correspondence should be addressed.
E-mail: seshim@inha.ac.kr

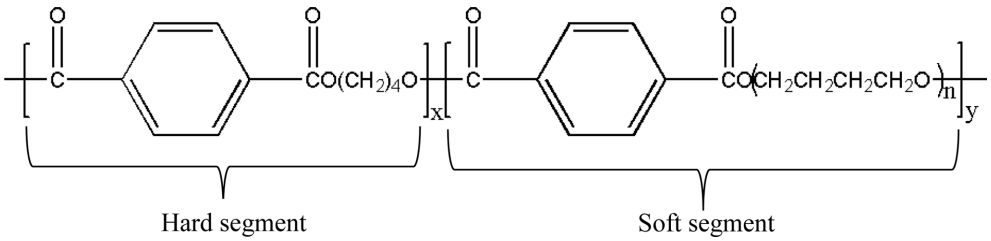

Figure 1. Chemical structure of thermoplastic polyester elastomer (TPEE).

manufacturing polymers with tailor-made properties. Nevertheless, the use of copolymerization is restricted because of its relatively high processing cost in industry.[3] As an alternative, blending of different two or more polymers has been a convenient and effective method for producing new polymeric materials from existing ones.[4-7] During the blending process, one polymer is dispersed mechanically inside the other polymer. The size and shape of the dispersed phase are influenced by the blending conditions, such as rheology, interfacial tension, and the composition of the blend.[8] The morphology of the interfaces between the dispersed and continuous phases has a critical influence on the mechanical properties of the multiphase blends.[8-12] Unfortunately, most polymers are not thermodynamically miscible with each other in blending situations.[13] Blending immiscible polymers does not normally result in a single-phase but in multi-phase blends. This leads to an unstable morphology, which will generate a blend with weak mechanical properties. In the past, many studies have attempted to control the morphology of immiscible polymer blends by introducing additives. As the additives used for this purpose, compatibilizers have been polymeric materials, such as graft or block copolymers, with functional groups that can interact with the constituents of a blend. Compatibilizers normally reduce the interfacial tension, increase the interface adhesion, and prevent the coalescence of a component in a blend. Therefore, they can contribute to provide immiscible polymer blends with compatibility and stabilize the morphology of a blend.[2,12-16] Tedesco *et al.*[17] analyzed the effects of maleic anhydride-grafted polypropylene (MA-*g*-PP) and glycidyl methacrylate-grafted polypropylene (GMA-*g*-PP) as compatibilizers on the morphology, mechanical and thermal properties of polypropylene(PP)/nylon 6 blends. MA-*g*-PP was found to be a more effective compatibilizer than GMA-*g*-PP in the PP/nylon6 system. Yoon *et al.*[18] compared the properties of poly(ethylene terephthalate) (PET)/PP blends with those of PET/MA-*g*-PP blends. It was reported that the reaction of ester groups of PET and maleic anhydride (MA) groups on MA-*g*-PP occurred in the PET/MA-*g*-PP blends.

Polypropylene (PP) is a widely used common thermoplastic because of its low cost, easy processability, and high rigidity.[19,20] In this study, PP was chosen as the counterpart to blending with TPEE in order to modify properties of TPEE. MA-*g*-PP was selected as a compatibilizer to present the components of the PP/TPEE blend with compatibility. MA is known to react with the carboxylic and/or hydroxyl end groups of the chain of the ester groups.[21-23] In the study, PP/TPEE blends with various ratios were prepared by melt- mixing in an internal mixer and the effect of the compatibilizers was investigated. Their morphology, thermal transition behavior, mechanical properties, and thermal stability were examined as a function of the TPEE and MA-*g*-PP contents.

Experimental

Materials. Polypropylene (J-150) was a homopolymer supplied by Lotte Chemical Corporation, Korea; its density was 0.90 g/cm^3 according to the ASTM D-792 and melt flow index (MFI) was 10 g/10 min at 230 °C and 2.16 kg by ASTM D-1238. The thermoplastic polyester elastomer (TRIEL 5300) was supplied by Samyang Corporation, Korea; its density was 1.1 g/cm^3 by ASTM D-792 and its MFI was 28-30 g/10 min at 230 °C and 2.16 kg by ASTM D-1238. Maleic anhydride-grafted PP (P MD353D) was obtained from DuPont, USA; its density was 0.9 g/cm^3 by ASTM D-792 and MFI was 22.7 g/10 min at 190 °C and 2.16 kg by ASTM D-1238.

Preparation of the Blends. To manufacture the PP and TPEE blends, neat PP and TPEE pellets were mixed by melt-mixing in a high viscosity kneader (internal mixer, TO-350, Test one) consisting of a co-rotating rotors. The PP and TPEE blends were prepared at a composition ratio of 90/10, 80/20, 70/30, and 60/40 weight percent (wt%) at 210 °C for 10 min. To characterize, after mixing, the blends were processed directly into the sheet by compressing in a hot-press at 190 °C for 2 min. The samples were dried in a vacuum oven at 25 °C

for 24 h. The PP/TPEE (80/20 wt%) blends with MA-*g*-PP were prepared under the above mentioned conditions. The MA-*g*-PP content in the PP/TPEE (80/20 wt%) blends was adjusted to 1.0, 3.0, 5.0, and 8.0 wt%. For comparison, the raw PP and TPEE sheets were prepared under the same processing conditions.

Characterization. The morphology of the pure PP and TPEE, PP/TPEE, and PP/TPEE/MA-*g*-PP blends was characterized using a field emission-scanning electron microscopy (FE-SEM, S-4300, Hitachi). For the FE-SEM observations, all the samples were immersed in liquid nitrogen and fractured, and their fractured cross-sections were investigated. The samples were sputter coated with Pt prior to analysis. The tensile tests were carried out using a universal testing machine (UTM 5569, Instron). The dumbbell-shaped specimens were prepared according to ASTM D-638 and characterized at a rate of 5 mm/min with a load cell of 50 kN. Notched Izod impact tests were conducted using an impact test instrument (Fractovis, Ceast) according to ASTM D-256. The specimens for the impact tests were rectangular bars, measuring 12.7 mm in width, 7.5 mm in thickness, and 63.6 mm in length. To characterize the thermal transition behavior of the PP, TPEE, PP/TPEE, and PP/TPEE blends including different MA-*g*-PP contents, a differential scanning calorimetry (DSC, Diamond TG/DTA Lab system, Perkin Elmer) was performed under a nitrogen atmosphere over the temperature range of -50~250 °C at a heating and cooling rate of 10 °C/min. The thermal degradation stability of the PP/TPEE/MA-*g*-PP blends was examined by thermogravimetric analysis (TGA, TA instrument, TA Q50) under a nitrogen atmosphere from 30 to 550 °C at a heating rate of 10 °C/min. The crystalline structure of the neat PP, TPEE, MA-*g*-PP, PP/TPEE (80/20 wt%) blend, and PP/TPEE (80/20 wt%) blends with different MA-*g*-PP contents was investigated using powder X-ray diffraction (Powder-XRD, DMAX 2500, RIGAKU).

Results and Discussion

Morphology. Figure 2 represents SEM microphotographs of the cross-section of the cryo-fractured PP, TPEE, and PP/TPEE blends. The neat PP showed an unevenly fractured surface due to its brittleness when broken quickly in the liquid nitrogen (Figure 2(a)), while the pure TPEE exhibited a relatively flat and smooth fractured surface owing to its ductile property (Figure 2(f)). In the case of the PP/TPEE blends, a separated-phase, namely sea-island morphology, was observed without miscibility between PP and TPEE (Figure 2(b)-(e)). In this morphology, PP and TPEE were considered to be the matrix and domain, respectively, considering the densities MFI values, and weight ratio of PP and TPEE. In addition, the mean size of the domain increased with increasing TPEE and decreasing PP content.

Figure 3 shows SEM images of a cross-section of the cryo-fractured PP/TPEE blends containing MA-*g*-PP. Spherical shapes of the TPEE domain in the SEM images were still faintly observed owing to the lack of compatibility between the

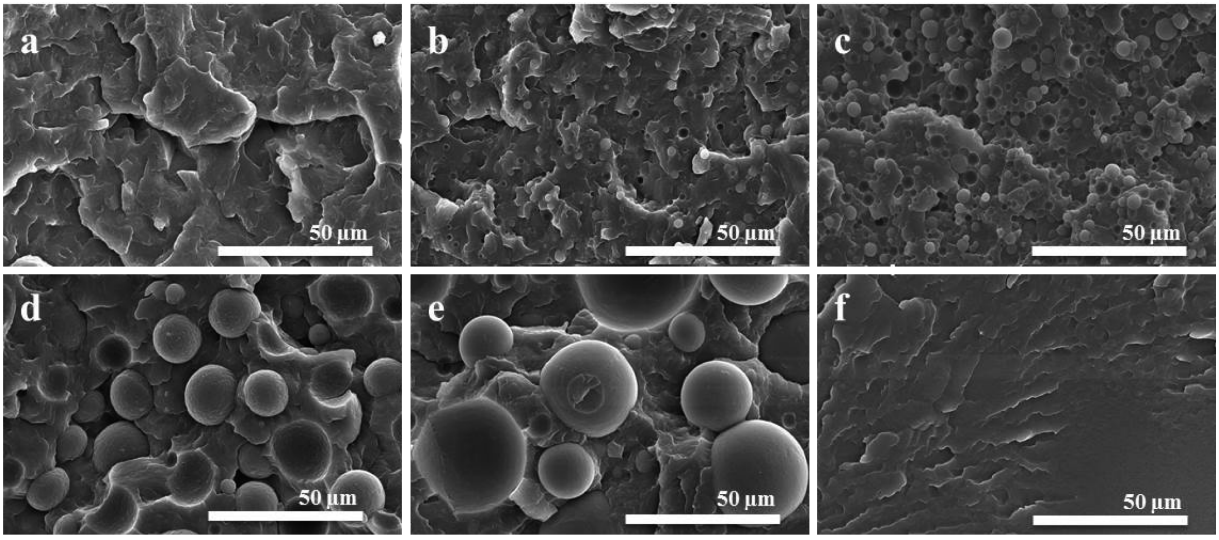

Figure 2. SEM microphotographs of the fractured surface of the PP/TPEE blends: (a) 100/0; (b) 90/10; (c) 80/20; (d) 70/30; (e) 60/40; (f) 0/100 wt%.

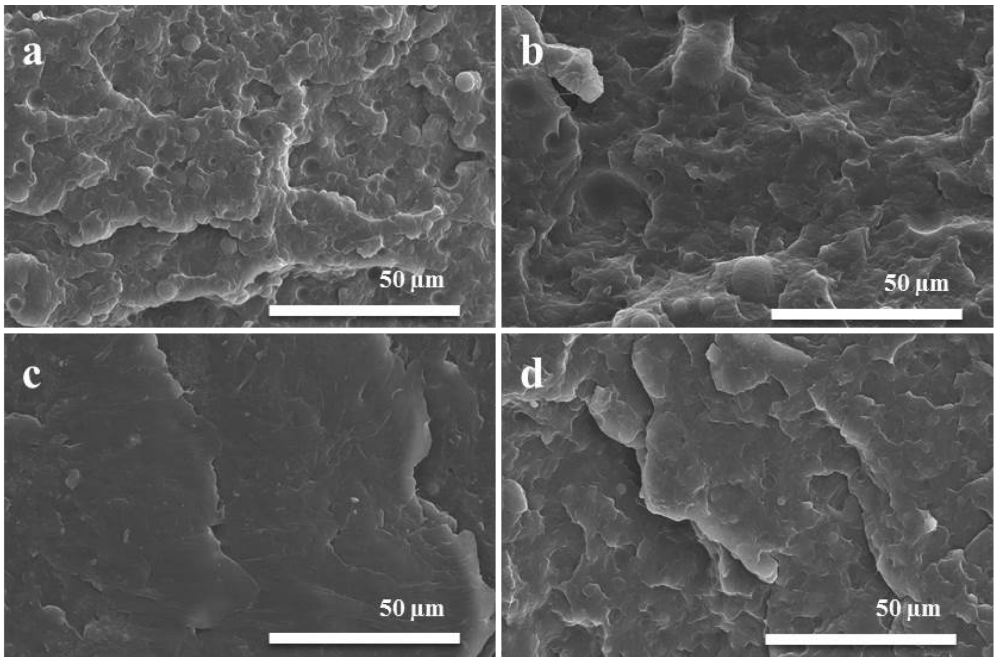

Figure 3. SEM microphotographs of the fractured surface of the PP/TPEE (80/20) blends with different MA-*g*-PP contents: (a) 1; (b) 3; (c) 5; (d) 8 wt%.

PP and TPEE, which resulted from 1 wt% of MA-*g*-PP (Figure 3(a)). With increment in MA-*g*-PP content, the spherical shape of the domain could not be discerned well and the fractured surface became flatter and smoother because of compatibility between PP and TPEE by MA-*g*-PP (Figure 3(b) and 3(c)). Champagne *et al*.[24] explained that the stable morphology made by the introduction of a compatibilizer was due to a decrease in interfacial tension obtained by the copolymer molecules generated *in-situ* on the blend interfaces and the copolymer layer was believed to prevent coalescence. On the other hand, at 8 wt% MA-*g*-PP, the domains were observed and the surface was not flat (Figure 3(d)). George *et al*.[11] reported that although the average domain size in the matrix of the blends was decreased by MA-*g*-PP, the further addition of MA-*g*-PP increased the average domain size in the matrix. They suggested that the increase in domain size above a certain amount of compatibilizer originates from the formation of micelles of compatibilizer in the continuous PP matrix. Several papers reported the critical micelle concentration (CMC) of the compatibilizer, which implies a critical amount of the compatibilizer required to saturate a unit volume of the interface, in addition, suggested that interfacial saturation of the binary polymer blends by the addition of compatibilizer had occurred over CMC.[25,26]

Mechanical Properties. Figure 4 presents the tensile tests of the PP, TPEE, and PP/TPEE blends at different TPEE contents and Figure 5 shows the tensile tests of the PP/TPEE (80/20 wt%) blends containing different MA-*g*-PP contents. In Figure 4(a), it was evaluated that the neat PP is the most brittle material of all the samples. Figure 4(b) shows that it has the highest tensile strength and the lowest elongation. In the stress-strain curves, the pure TPEE was not broken owing to its high elasticity and the addition of TPEE significantly changes the mechanical properties of the PP/TPEE blends. The curves indicate that with increasing TPEE content, the tensile strength and Young's modulus of the PP/TPEE blends decreased and the elongation of those increased. Martuscelli *et al*.[27] reported that the spherulite growth of PP in the blends with rubber was inhibited by the existence of a rubber phase. George *et al*.[11] reported that the decrease in tensile strength and Young's modulus at the PP/nitrile rubber (NBR) blends with increasing NBR contents was due to the presence of a soft rubber phase and a decrease in crystallinity of the PP phase. In our DSC measurement, it was observed that the crystallinity (X_c) of the PP/TPEE blends is truly decreased at the PP/TPEE blends with increasing TPEE content (Table 1). Therefore, the decrease in tensile strength, Young's modulus and increase in elongation of PP/TPEE blends with the addition of TPEE are due to the presence of a soft TPEE phase and a decrease in crystallinity of the PP/TPEE blends.

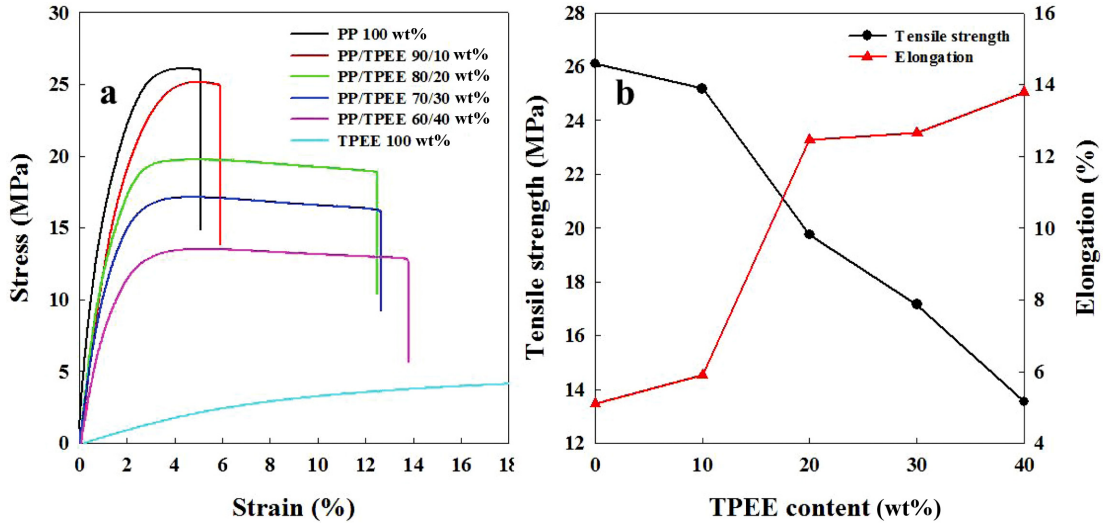

Figure 4. (a) Strain-stress curves; (b) tensile strength and elongation of the PP/TPEE blends.

Table 1. Heat of Fusion and Crystallinity of the PP/TPEE Blends

PP/TPEE (wt%)	100/0	90/10	80/20	70/30	60/40
ΔH_f (J/g)	104.69	93.73	83.06	67.50	56.10
X_c (%)	75.92	75.52	75.29	69.92	67.8

In Figure 5(a), the stress-strain curves of PP/TPEE (80/20 wt%) blends with different MA-*g*-PP contents are presented. With increasing MA-*g*-PP concentration as a compatibilizer in the PP/TPEE blend, the tensile strength increased up to a MA-*g*-PP concentration of 5 wt%, but decreased at 8 wt% of MA-*g*-PP. The tendency of the tensile strength was explained by the morphology revealed by SEM. With increase in MA-*g*-PP content, the morphology of PP/TPEE/MA-*g*-PP became more stable than that of the PP/TPEE blend (Figure 2(c) and Figure 3(a)-(c)). In the case of the PP/TPEE blend with 8 wt% of MA-*g*-PP, the morphology was slightly less stable than that of the PP/TPEE blend with 5 wt% of MA-*g*-PP (Figure 3(d)). Therefore, it is presumed that tensile strength is fairly reliant on the stability of the morphology.

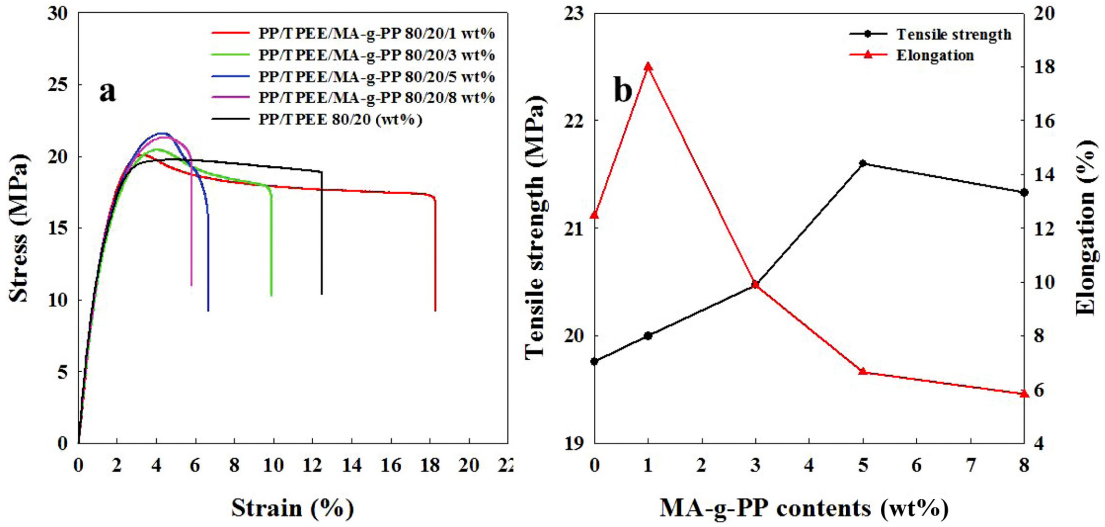

Figure 5. (a) Strain-stress curves; (b) tensile strength and elongation of the PP/TPEE (80/20 wt%) blends with different MA-*g*-PP contents.

The impact strength of the PP, TPEE, PP/TPEE blends, and PP/TPEE (80/20 wt%) blends at different MA-*g*-PP contents is shown in Figure 6. In Figure 6(a), it is observed that the impact strength of the PP/TPEE blends increases significantly up to 20 wt% of TPEE, and decreases gradually at higher concentrations. It is assumed that the impact strength of PP/TPEE blends depends partially on the extent of the crystallinity of PP phase. Figure 6(b) compares the impact strength of the PP/TPEE (80/20 wt%) blends containing MA-*g*-PP with the PP/TPEE blend. The value of PP/TPEE/MA-*g*-PP blends was much higher than that of the PP/TPEE (80/20 wt%) blend without MA-*g*-PP. This indicates that the compatibility by MA-*g*-PP has an effect on the toughness of the PP/TPEE blends. However, at 8 wt% of MA-*g*-PP, the impact strength of PP/TPEE blend decreased. This was attributed to the unstable morphology caused by the formation of compatibilizer micelles in the continuous PP phase.

XRD Analysis. Figure 7 shows X-ray diffraction (XRD) patterns of the neat PP, TPEE, MA-*g*-PP, PP/TPEE blend, and blends with different MA-*g*-PP contents. The PP displayed several sharp diffraction peaks at around 2θ = 13.9, 16.6, 18.3, 20.9, and 21.6° (Figure 7(A)). The XRD peaks of the PP cor-

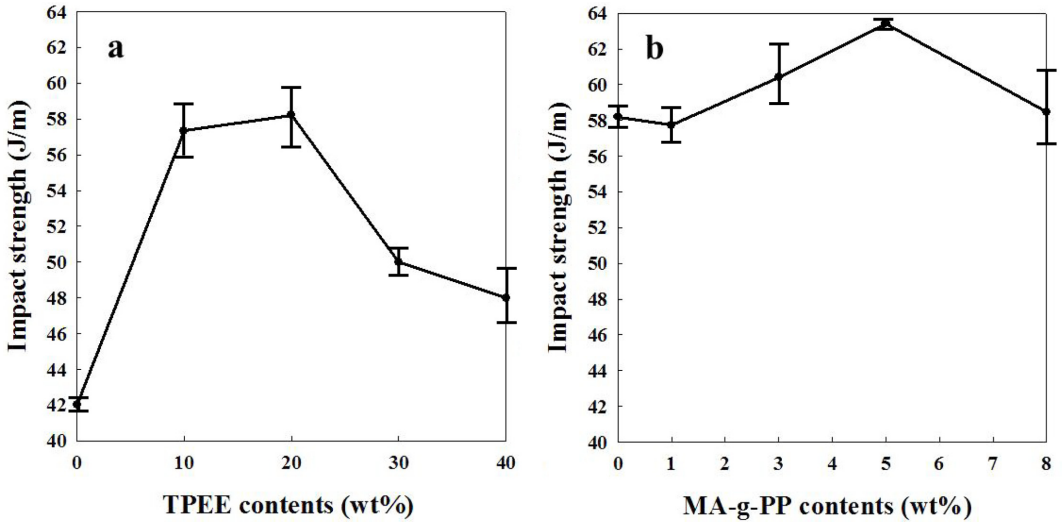

Figure 6. Impact strength of (a) PP/TPEE blends; (b) PP/TPEE (80/20) blends with different MA-*g*-PP contents.

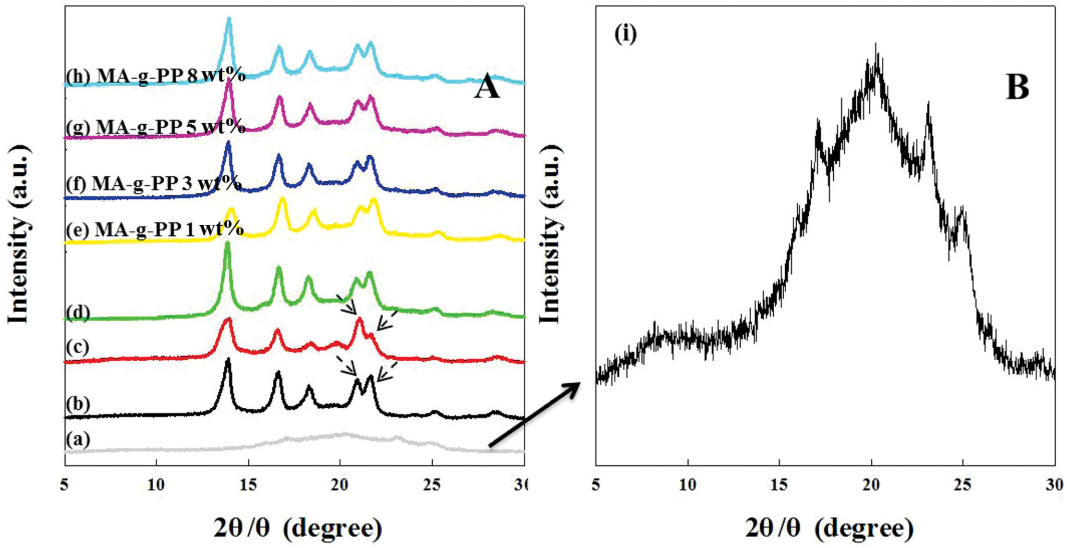

Figure 7. XRD patterns of (a) TPEE; (b) PP; (c) MA-*g*-PP; (d) PP/TPEE (80/20) blend; (e-h) PP/TPEE (80/20) blend with different MA-*g*-PP contents; (i) extended XRD patterns of TPEE.

respond to the α-form crystals, which form rapidly because of its fast crystallization rate during the melt-quenching process.[4] In Figure 7(B), the TPEE exhibited very weak diffraction peaks at about 2θ = 15.9, 17.0, 20.3, 23.0, and 24.9° which were assigned to the reflections of the crystalline poly(butylene terephthalate) (PBT) segments in TPEE.[28] The intensity of XRD peaks of the TPEE was too weak to identify the peak of the PP/TPEE blends (Figure 8(a)). In other words, it was conformed that the sharp XRD peaks of the PP/TPEE (80/20 wt%) blends were attributed to the PP with α-form crystals. The sharp XRD peaks of the MA-*g*-PP were similar to those of the neat PP. On the other hand, the peaks of the MA-*g*-PP, at 20.9° and 21.6° showed contrary results to that of the PP, i.e., the intensity of the peak at 20.9° of the MA-*g*-PP was higher than that of the peak at 21.6° of the MA-*g*-PP. In contrast, the intensity of the peaks of the PP at 20.9° and 21.6° was reversed. In the PP/TPEE (80/20 wt%) blends with MA-*g*-PP, the intensity of 20.9° peak was strengthened and that of the 21.6° peak was weakened gradually due to the effects of MA-*g*-PP (Figure 7(A)).

Thermal Transition and Crystallization. Figure 8 exhibits DSC thermograms of the second heating scan of the melt-quenched PP, TPEE, PP/TPEE blends, and PP/TPEE/MA-*g*-PP blends. Figure 8(a) shows that the neat TPEE showed a weak glass transition temperature (T_g) at 4 °C without displaying the meting point (T_m). Therefore, it is considered that TPEE is in amorphous state. The neat PP exhibited only a sharp melting transition (T_m) at 165 °C without showing a glass transition. Lee *et al.*[4] reported that the melt-quenched PP without its glass transition temperature (T_g) and cold-crystallization at the DSC thermograms is related with semi-crystalline state with its rapid crystallization rate. For the PP/TPEE blends, the melting temperature (T_m) and glass transition temperature (T_g) were detected at approximately 163 and 3 °C, respectively. It is indicated that the melting temperature is related to the melt transition of the neat PP and glass transition temperature of the blends are consistent with the glass transition of the neat TPEE constituent in the blends. The crystallinity (X_c) of the PP, TPEE, and PP/TPEE blends was calculated using the following eq. (1) (Table 1):

$$X_c = \frac{\Delta H_f}{\Delta H_f^o w} \times 100 \quad (1)$$

where ΔH_f is the heat of fusion of the PP and PP/TPEE blends, ΔH_f^o is 137.9 J/g, as the heat of fusion for the pure PP with 100% crystallinity,[29] and w is the mass fraction of PP in the blend. The crystallinity (X_c) of the PP/TPEE blends decreased with increasing TPEE content.

In the thermograms (Figure 8(b)), the melt-quenched PP/TPEE/MA-*g*-PP blends represented a weak glass transition (T_g) peak, which shifted gradually to a lower temperature in accordance with higher amount of MA-*g*-PP. The melting temperature (T_m) of the PP/TPEE/MA-*g*-PP blends declined due to

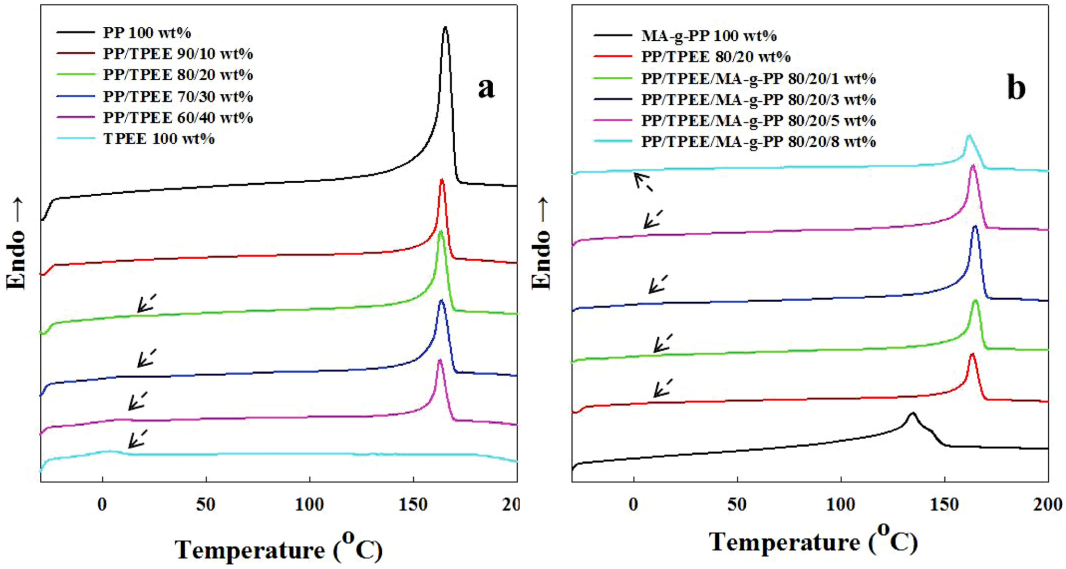

Figure 8. DSC thermograms of the second heating scan for (a) PP, TPEE, and PP/TPEE blends; (b) MA-*g*-PP and PP/TPEE (80/20) blends with different MA-*g*-PP contents.

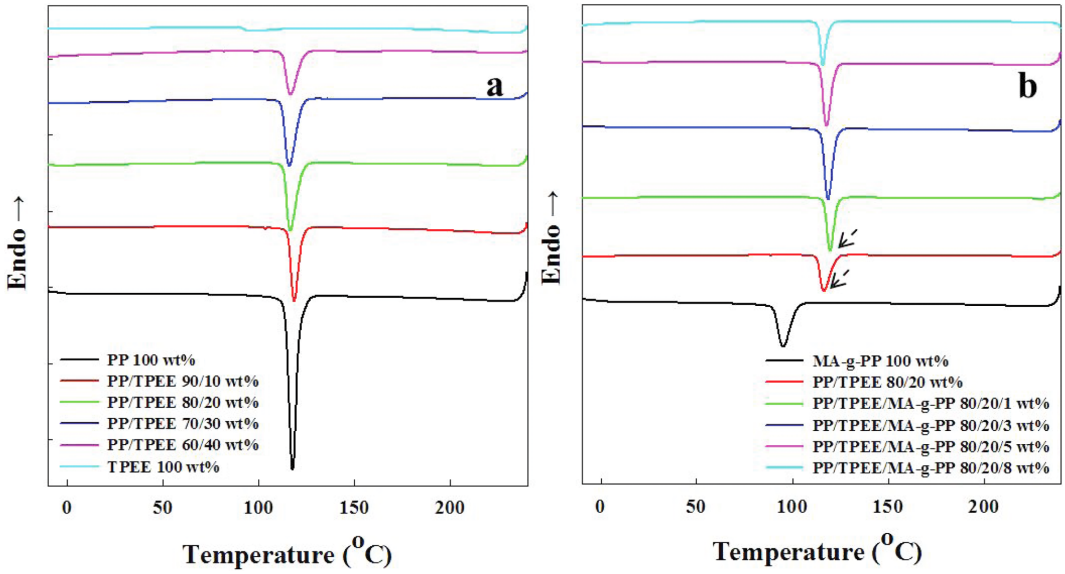

Figure 9. DSC thermograms of the second cooling scan for (a) PP, TPEE, and PP/TPEE blends; (b) MA-*g*-PP and PP/TPEE (80/20) blends with different MA-*g*-PP contents.

the increase in MA-*g*-PP which exhibits a low melting temperature (T_m).

Figure 9 shows the DSC thermograms of the second cooling scan of the melt-quenched PP, TPEE, PP/TPEE blends and PP/TPEE/MA-*g*-PP blends. In the thermograms (Figure 9(a)), the neat PP displayed a definite crystallization temperature (T_c) at 120 °C, whereas the neat TPEE did not indicate the crystallization temperature (T_c). The crystallization temperature (T_c) of the PP/TPEE blends moved toward a lower temperature, which is due to a decrease in the crystallization rate caused by the larger TPEE amount. In the thermograms (Figure 9(b)), the crystallization temperature (T_c) of the PP/TPEE blends with 1 wt% MA-*g*-PP shifted to higher temperature compared to the that of the PP/TPEE blend, which is induced by the faster crystallization rate of the PP/TPEE/MA-*g*-PP blend than that of the PP/TPEE (80/20) blend owing to the introduction of MA-*g*-PP. On the other hand, the crystallization temperature (T_c) of the PP/TPEE/MA-*g*-PP blends diminished with increasing MA-*g*-PP content, which showed a low crystallization temperature (T_c).

Thermal Stability. Figure 10 shows the TGA thermograms of the PP, TPEE, PP/TPEE blend, and PP/TPEE blends according to the different MA-*g*-PP contents, which were measured under a nitrogen atmosphere. The thermal stability and temperature for the start of degradation of the pure PP was far higher than of that of the neat TPEE. The thermal degradation stability of the PP/TPEE (80/20 wt%) blend showed a value

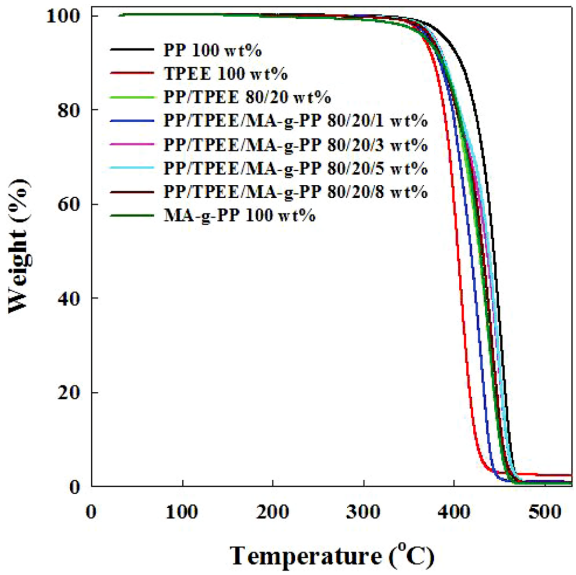

Figure 10. TGA thermograms of PP, TPEE, PP/TPEE, and PP/TPEE/MA-*g*-PP blends.

intermediate between those of TPEE and PP. The thermal stability and degradation rate of the pristine MA-*g*-PP was similar to that of the PP/TPEE (80/20 wt%) blend. It is reported that the thermal stability of the MA-*g*-PP is low in comparison to the neat PP because of the presence of MA groups on the PP chains.[30] For precise analysis, Table 2 lists the residual weight percent of all samples at 370, 400, and 430 °C. As expected, the residual weight of the neat PP and TPEE at 370, 400, and

Table 2. Thermal Degradation Stability of the PP, TPEE, PP/TPEE Blend, and PP/TPEE/MA-*g*-PP Blends

PP/TPEE/MA-*g*-PP (wt%)	PP	TPEE	MA-*g*-PP	80/20/0	80/20/1	80/20/3	80/20/5	80/20/8
Weight (%) at 370 °C	98	94	94.9	96.9	95.7	97	96.9	96.4
Weight (%) at 400 °C	92.7	60.7	83	82.7	78.2	83.4	84	82.8
Weight (%) at 430 °C	72.8	6	47.8	47	27.3	58.8	62.2	54.8

430 °C was the highest and lowest, respectively. In the case of the PP/TPEE/MA-*g*-PP blends except for 1 wt% MA-*g*-PP, the residual weight figures were higher than those of the PP/TPEE (80/20) blend. In addition, for the PP/TPEE/MA-*g*-PP blend, an increase in the MA-*g*-PP contents tended to enhance the thermal stability and degradation rate of the blends. Consequently, the slightly better thermal stability of the PP/TPEE/MA-*g*-PP blends with increasing MA-*g*-PP was due to the compatibility between the PP and TPEE.

Conclusions

In this study, immiscible PP/TPEE blends and blends with MA-*g*-PP concentrations ranging from 0 to 8 wt% were prepared through convenient and efficient melt-mixing using an internal mixer. The morphology of a series of PP/TPEE blend suggested that TPEE was dispersed in the continuous PP matrix and was immiscible with each other. In addition, the morphology of the PP/TPEE/MA-*g*-PP showed that the PP and TPEE were compatible because MA-*g*-PP served as an effective compatibilizer. The tensile tests showed that with increasing TPEE content, the tensile strength and Young's modulus of the PP/TPEE blends decreased and the elongation of those increased. The tensile strength of the PP/TPEE/MA-*g*-PP improved up to 5 wt% MA-*g*-PP, however decreased at 8 wt% of MA-*g*-PP, which is associated with the morphology, as confirmed by the morphology. The impact tests exhibited that the impact strength of the PP/TPEE blends and the PP/TPEE/MA-*g*-PP was enhanced by TPEE and MA-*g*-PP, respectively. XRD confirmed that PP displayed strong peaks in the blends owing to the α-form crystals, and for the PP/TPEE/MA-*g*-PP blends, the intensity of the 20.9 and 21.6° peaks became stronger and gradually weaker, respectively, due to the effect of the MA-*g*-PP. DSC showed that the crystallinity (X_c) of the PP/TPEE blends decreased with increasing TEPP content and the PP/TPEE/MA-*g*-PP blends presented that a single weak glass transition (T_g) peak changed according to the mixing ratio caused by the compatibility between the PP and TPEE. The thermal stability of the PP/TPEE blends with MA-*g*-PP was higher than that of the PP/TPEE blend because of the action of the compatibility between PP and TPEE. As a total result of this study, it was sound to confirm that improved morphology, mechanical properties, thermal degradation stability, and changed crystallinity of the PP/TPEE blend were due to the existence of compatibility between PP and TPEE due to a compatibilizer.

Acknowledgement. This study was supported by a grant (10046535) from the Korea Ministry of Trade, Industry and Energy (MOTIE), Republic of Korea (2014).

References

1. H. U. Zaman, J. C. Song, L. Park, I. Kang, S. Park, G. Kwak, B. Park, and K. Yoon, *Polym. Bull.*, **67**, 187 (2011).
2. Y. Nagai, T. Ogawa, L.Y. Zhen, Y. Nishimoto, and F. Ohishi, *Polym. Degrad. Stabil.*, **56**, 115 (1997).
3. H. H. Ismail and M. Nasir, *Polym. Test.*, **21**, 163 (2002).
4. T. W. Lee and Y. G. Jeong, *Compos. Sci. Technol.*, **103**, 78 (2014).
5. M. Palabiyik and S. Bahadur, *Wear*, **246**, 149 (2000).
6. Y. Zhang, M. Zuo, Y. Song, X. Yan, and Q. Zheng, *Compos. Sci. Technol.*, **106**, 39 (2015).
7. B. G. Girija, R. R. N. Sailaja, and G. Madras, *Polym. Degrad. Stab.*, **90**, 147 (2005).
8. U. Sundararaj and C. W. Macosko, *Macromolecules*, **28**, 2647 (1995).
9. A. M. C. Souza and N. R. Demarquette, *Polymer*, **43**, 3959 (2002).
10. S. N. Sathe, S. Devi, G. S. S. Rao, and K. V. Rao, *J. Appl. Polym. Sci.*, **61**, 97 (1996).
11. S. George, R. Joseph, and S. Thomas, *Polymer*, **36**, 4405 (1995).
12. Y. Wang, Q. Zhang, and Q. Fu, *Macromol. Rapid Commun.*, **24**, 231 (2003).
13. K. Wallheinke, P. Potschke, and H. Stutz, *J. Appl. Polym. Sci.*, **65**, 2217 (1997).
14. M. Yazdani-pedra, H. Vega, J. Retuert, and R. Quijada, *Polym. Eng. Sci.*, **43**, 960 (2003).
15. J. Duvall, C. Sellitti, C. Myers, A. Hiltner, and E. Baer, *J. Appl. Polym. Sci.*, **52**, 195 (1994).
16. J. Roeder, R. V. B. Oliveira, M. C. Goncalves, V. Soldi, and A.

T. N. Pires, *Polym. Test.*, **21**, 815 (2002).
17. A. Tedesco, R. V. Barbosa, S. M. B. Nachtigall, and R. S. Mauler, *Polym. Test.*, **21**, 11 (2002).
18. K. H. Yoon, H. W. Lee, and O. O. Park, *J. Appl. Polym. Sci.*, **70**, 389 (1998).
19. S. Bagheri-Kazemabad, D. Fox, Y. Chen, L. M. Geever, A. Khavandi, R. Bagheri, C. L. Higginbotham, H. Zhang, and B. Chen, *Compos. Sci. Technol.*, **72**, 1697 (2012).
20. Y. X. Pang, D. M. Jia, H. J. Hu, D. J. Hourston, and M. Song, *Polymer*, **41**, 357 (2000).
21. J. Lepers, B. D. Favis, and C. Lacroix, *J. Appl. Polym. Sci.*, **37**, 939 (1999).
22. Y. Sun, G. Hu, M. Lambla, and H. K. Kotlar, *Polymer*, **18**, 4119 (1996).
23. W. Loyens and G. Groeninckx, *Macromol. Chem. Phys.*, **203**, 1702 (2002).
24. M. F. Champagne, M. A. Huneault, C. Roux, and W. Peyrel, *Polym. Eng. Sci.*, **39**, 976 (1999).
25. S. Thomas and R. E. Prud'homme, *Polymer*, **33**, 4260 (1992).
26. J. M. Willis, B. D. Favis, and J. Lunt, *Polym. Eng. Sci.*, **30**, 1073 (1990).
27. E. Martuscelli, C. Silvestre, and G. Abate, *Polymer*, **23**, 229 (1982).
28. Y. Bai, S. Lv, F. Liu, and M. T. Run, *J. Macromol. Sci.- Phys.*, **53**, 1553 (2014).
29. P. V. Joseph, K. Joseph, S. Thomas, C. K. S. Pillai, V. S. Prasad, G. Groeninckx, and M. Sarkissova, *Compos. Part A: Appl. Sci. Manuf.*, **34**, 253 (2003).
30. G. S. Ezat, A. L. Kelly, S. C. Mitchell, M. Youseffi, and P. D. Coates, *Polym. Compos.*, **33**, 1376 (2012).